An Informatics-assisted Label-free Approach for Personalized Tissue Membrane Proteomics: Case Study on Colorectal Cancer*⑤

Chia-Li Han‡[h], Jinn-Shiun Chen§¶[h], Err-Cheng Chan‖[h], Chien-Peng Wu‡, Kun-Hsing Yu, Kuei-Tien Chen‖, Chih-Chiang Tsou‡‡, Chia-Feng Tsai‡, Chih-Wei Chien§§, Yung-Bin Kuo¶¶, Pei-Yi Lin‡, Jau-Song Yu‖‖[a], Chuen Hsueh‖‖[b], Min-Chi Chen[c], Chung-Chuan Chan[d], Yu-Sun Chang‖‖[e], and Yu-Ju Chen‡[f,g]**

We developed a multiplexed label-free quantification strategy, which integrates an efficient gel-assisted digestion protocol, high-performance liquid chromatography tandem MS analysis, and a bioinformatics alignment method to determine personalized proteomic profiles for membrane proteins in human tissues. This strategy provided accurate (6% error) and reproducible (34% relative S.D.) quantification of three independently purified membrane fractions from the same human colorectal cancer (CRC) tissue. Using CRC as a model, we constructed the personalized membrane protein atlas of paired tumor and adjacent normal tissues from 28 patients with different stages of CRC. Without fractionation, this strategy confidently quantified 856 proteins (≥2 unique peptides) across different patients, including the first and robust detection (Mascot score: 22,074) of the well-documented CRC marker, carcinoembryonic antigen 5 by a discovery-type proteomics approach. Further validation of a panel of proteins, annexin A4, neutrophils defensin A1, and claudin 3, confirmed differential expression levels and high occurrences (48–70%) in 60 CRC patients. The most significant discovery is the overexpression of stomatin-like 2 (STOML2) for early diagnostic and prognostic potential. Increased expression of STOML2 was associated with decreased CRC-related survival; the mean survival period was 34.77 ± 2.03 months in patients with high STOML2 expression, whereas 53.67 ± 3.46 months was obtained for patients with low STOML2 expression. Further analysis by ELISA verified that plasma concentrations of STOML2 in early-stage CRC patients were elevated as compared with those of healthy individuals ($p < 0.001$), suggesting that STOML2 may be a noninvasive serological biomarker for early CRC diagnosis. The overall sensitivity of STOML2 for CRC detection was 71%, which increased to 87% when combined with CEA measurements. This study demonstrated a sensitive, label-free strategy for differential analysis of tissue membrane proteome, which may provide a roadmap for the subsequent identification of molecular target candidates of multiple cancer types. *Molecular & Cellular Proteomics 10: 10.1074/ mcp.M110.003087, 1–15, 2011.*

From the ‡Institute of Chemistry, Academia Sinica, Taipei 11529, Taiwan; §Colorectal Section, Department of Surgery, Chang Gung Memorial Hospital, Taoyuan 33305, Taiwan; ¶School of Medicine, Chang Gung University, Taoyuan 33302, Taiwan.; ‖Department of Medical Biotechnology and Laboratory Science, Chang Gung University, Taoyuan 33302, Taiwan; **College of Medicine, National Taiwan University, Taipei 10002, Taiwan; ‡‡Institutes of Information Science, Academia Sinica, Taipei 11529, Taiwan; §§Department of Chemistry, National Tsing Hua University, Hsinchu 30013, Taiwan; ¶¶College of Biological Science and Technology, National Chiao Tung University, Hsinchu 30013, Taiwan; ‖‖Molecular Medicine Research Center, Chang Gung University, Taoyuan 33302, Taiwan; [a]Department of Cell and Molecular Biology, Chang Gung University, Taoyuan 33302, Taiwan; [b]Department of Pathology, Chang Gung Memorial Hospital, Taoyuan 33305, Taiwan; [c]Public Health and Biostatistics Consulting Center, Chang Gung University, Taoyuan 33302, Taiwan; [d]Department of Gastroenterology, Hsinchu Cathay General Hospital, Hsinchu 30013, Taiwan; [e]Graduate Institute of Biomedical Sciences, School of Medicine, Chang Gung University, Taoyuan 33302, Taiwan; [f]Institute of Chemistry, Academia Sinica, Taipei 11529, Taiwan; [g]Department of Chemistry, National Taiwan University, Taipei 10689, Taiwan.

Colorectal cancer (CRC)[1] is one of the most prevalent cancers and the fourth leading cause of cancer mortality worldwide, with an estimated 1,000,000 new cases and ~500,000 related deaths every year (1, 2). Detection of CRC and subsequent intervention at an earlier stage has the potential to reduce both incidence and mortality of the disease (3, 4). Clinically, colonoscopy represents the most sensitive approach for early detection among various screening tests. However, only 39% CRC patients are diagnosed at a localized stage by the invasive colonoscopy (2, 5); most of the patients

[1] The abbreviations used are: CRC, colorectal cancer; S.D., standard deviation; ANXA4, annexin A4; DEFA1, neutrophil defensin A1; CLDN3, claudin 3; STOML2, stomatin-like 2; CEA, carcinoembryonic antigen; IHC, immunohistochemical staining; XIC, extracted ion chromatography; ROC, receiver operating characteristic; AUC, the area under the ROC curve.

are diagnosed at advanced stages. At the level of molecular diagnosis, at present, carcinoembryonic antigen (CEA) is the most widely used serum tumor marker for CRC (6–8). Because of its low sensitivity and specificity at early cancer stage, CRC screening based on serum and plasma levels of the CEA biomarker is only recommended for prognostic use (8). Therefore, development of better tumor markers aimed at early detection of CRC would improve the diagnosis and/or monitoring of CRC.

Proteomics technology is a powerful tool for uncovering aberrant protein profiles of clinical samples (9, 10). It has been hypothesized that the concentrations of potential biomarkers are highest in the tumor and its immediate microenvironment (*i.e.* tissue interstitial fluid) (11). If a protein is up-regulated in cancer cells, cancer tissue should possess higher concentration of the protein than serum does. Therefore, many efforts have been made to map the specific genotyping of expressed genes or proteins in the cancerous tissues (12–14), including the most comprehensive human protein atlas for normal and cancer tissues to date (15, 16). Among published CRC-related proteomics literature, the most widely used proteomics approach for identification of differentially expressed proteins in individual CRC patient was based on two-dimensional (2D) PAGE and the more sophisticated technique of two-dimensional differential gel electrophoresis coupled with MS (17–24). By analyzing paired tumor and adjacent normal tissues from patients, these gel-based methods have led to discovery of a variety of proteins involving in signal transduction, cellular reorganization, and tissue hypoxia as potential biomarkers for CRC. Alfonso *et al.* (25) analyzed the membrane fractions of six paired CRC mucosal tissues using two-dimensional differential gel electrophoresis analysis, identifying annexin A2, annexin A4 (ANXA4) and VDAC as potential markers for CRC diagnosis and, presumably, therapy. In a recent study, Ma *et al.* (20) found elevated expression of desmin from fetal colorectal tissues and paired CRC tumor-adjacent normal tissues using 2D-PAGE. Up-regulation of oncofetal desmin is correlated with the severity and differentiation of CRC and with poor survival. Thus, desmin could be considered a potential oncofetal serum tumor marker for CRC (20). Although 2D-PAGE is capable of analyzing differentially expressed proteins, this method has limited dynamic range, lower throughput and lower sensitivity to analyze hydrophobic proteins or low-abundance proteins. To the best of our knowledge, the current clinically used CRC marker, CEA (also named carcinoembryonic antigen-related cell adhesion molecule 5, CEACAM5, a membrane protein), has not been identified using the above proteomics methodologies.

Dysregulation of membrane proteins has been linked to a variety of human cancers (26, 27). Most of the FDA-approved cancer biomarker, such as CEA and CA19–9, and ~70% of all known pharmaceutical drug targets are mainly membrane proteins (28). Thus, precise and in-depth characterization of membrane proteins in tumors and adjacent normal tissues

from patients will facilitate our understanding of the roles of these proteins in regulating biological processes, which will ultimately provide more reliable biomarker candidates for diagnosis and prognosis, and may contribute to a personalized treatment approach for individual patients. Despite the promise of membrane proteomics for disease marker discovery, only a few studies (29, 30) have characterized the tissue membrane proteome because of the difficulty and inherent challenges of membrane protein analysis and limited amounts of human tumor samples.

In this study, we present a multiplexed label-free quantitation strategy to characterize the individual membrane proteomic profiles in human tissues. This strategy integrates an efficient gel-assisted digestion protocol (31), high-performance liquid chromatography tandem MS (LC-MS/MS) analysis, and a bioinformatics alignment method (32) in attempt to comprehensively map and accurately quantify the membrane proteome. Using CRC as a model to discover potential biomarkers for diagnosis, we applied this strategy to the analysis of differentially expressed membrane proteins in tumor and adjacent normal tissues from each CRC patient. Twenty-eight paired tumor and adjacent normal tissues from patients in Dukes' A ($n = 4$), Dukes' B ($n = 7$), Dukes' C ($n = 11$) and Dukes' D ($n = 6$) stages were analyzed. We addressed two issues. (1) From the technical prospective, can this approach provide good sensitivity for robust identification of the current CRC protein biomarker, CEA (CEACAM5)? (2) More importantly, can the technological advancement lead to discovery of additional proteins that are involved in colon tumorigenesis and that can serve as new diagnostic and prognostic protein biomarkers? Contrary to most previous studies using pooled tissue samples, the individual paired-tissue comparisons used here provide information concerning biological and genetic variations between different individuals. The high-throughput strategy is also advantageous in that it provides an analysis of individual proteomic patterns among patients to evaluate the heterogeneity of tissues profiles.

In addition to the confident identification of CEA in the 28 patients, this study identified a panel of membrane proteins with high levels of elevated expression levels in CRC patients. To further evaluate the clinical relevance of these candidates, their expression levels in tissue or serum were examined by Western blot, immunohistochemical staining, ELISA, and clinicopathologic analysis from a large cohort of patients with known clinical outcomes. The results demonstrated the power of tissue membrane proteomics for the discovery of valuable biomarker candidates for early diagnosis and prognosis of CRC.

EXPERIMENTAL PROCEDURES

Materials—Protease inhibitor was obtained from Merck (Darmstadt, Germany). Monomeric acrylamide/bisacrylamide solution (40%, 29:1) was purchased from Bio-Rad (Hercules, CA). Trypsin (modified, sequencing grade) was obtained from Promega (Madison, WI). The BCA and Bradford protein assay reagent kits were

obtained from Pierce (Rockford, IL). SDS was purchased from GE Healthcare (Central Plaza, Singapore). Ammonium persulfate (APS) and *N,N,N′,N′*-tetramethylethylenediamine (TEMED) were purchased from Amersham Biosciences (Piscataway, NJ). Tris(2-carboxyethyl)phosphine hydrochloride (TCEP), triethylammonium bicarbonate (TEABC), methyl methanethiosulfonate (MMTS), trifluoroacetic acid (TFA), sodium carbonate (Na_2CO_3), sucrose, Tris-HCl, NaCl, $MgCl_2$, and HPLC-grade acetonitrile (ACN) were purchased from Sigma-Aldrich (St. Louis, MO). Formic acid (FA) was purchased from Riedel de Haen (Seelze, Germany). Water was obtained from a Milli-Q Ultrapure Water Purification System (Millipore, Billerica, MA).

Patients and Specimen Collection—Clinical tissue samples were obtained from Chang Gung Memorial Hospital at Lin-Kou, Taiwan in accordance with approved human subject guidelines authorized by Medical Ethics and Human Clinical Trial Committee at Chang Gung Memorial Hospital. Following surgery, the tumor and adjacent normal tissues were collected in separate tubes, kept on dry ice for 30 min during transportation, and stored at −80 °C before further processing. Adjacent normal tissue was obtained from the distal edge of the resection ≥10 cm from the tumor. In the discovery phase, a total of 28 pairs of cancerous and adjacent normal tissue were collected and analyzed from individual patients with Dukes' A ($n = 4$), Dukes' B ($n = 7$), Dukes' C ($n = 11$) or Dukes' D ($n = 6$) stages CRC patients (supplemental Table 1). In the validation phase, 205 colorectal carcinomas patients and 140 blood samples without hemolysis or lipemia, including 70 samples from CRC patient and 70 age-matched individuals without CRC, were collected from the Department of Colorectal Cancer, Chang Gung Memorial Hospital (33). All CRC patients had histologically verified adenocarcinoma of the colon or rectum that was confirmed by pathologists. Patient characteristics were obtained from pathology records. Subjects with a history of other malignant diseases or infectious disease, or who had undergone surgery 6 months prior to the start of this research were excluded for this retrospective study. Fresh plasma samples were obtained before surgery and were stored at −80 °C until use.

Purification of Membrane Protein Fraction from Paired Normal and Tumor Tissues of 28 Patients—Frozen tissues were thawed rapidly at 37 °C, cut into small pieces, and washed by 0.9% NaCl to remove blood. The precleaned tissues were homogenized in STM solution (5 ml/g tissue, 0.25 M sucrose, 10 mM Tris-HCl, and 1 mM $MgCl_2$) with protease inhibitor mixture (100:1, sample/protease inhibitor, v/v, Calbiochem) using homogenizer mechanism (Polytron System PT 1200 E, Luzernerstrasse, Switzerland). Nuclei and tissue debris were removed by centrifugation ($260 \times g$) for 5 min at 4 °C. The supernatant was first centrifuged at $1500 \times g$ for 10 min at 4 °C to pellet the crude membrane proteins. The pellet was mixed with two-thirds of the original homogenate volume (0.25 M STM solution with protease inhibitor mixture) and then centrifuged at $16,000 \times g$ for 1 h at 4 °C to purify the membrane pellet. The pellet was washed in 1 ml of 0.1 M Na_2CO_3 for overnight at 4 °C and re-collected by centrifugation at $16,000 \times g$ for 1 h at 4 °C. The purified membrane pellet was dissolved in 50 μl of 90% (v/v) FA prior to the Bradford assay to determine the membrane protein concentration and then was vacuum dried and stored at −80 °C for further processing.

Gel-assisted Digestion of Membrane Proteins—The membrane protein pellet was subjected to our previously reported gel-assisted digestion (31). In brief, membrane protein pellet was resuspended in 6 M urea, 5 mM EDTA, and 2% (v/v) SDS in 0.1 M TEABC and sonicated by a Bioruptor (Diagenode, Belgium) at 4 °C for 10 min. Bovine serum Albumin (BSA) was added as internal standard (1000:1, protein/BSA, w/w). Proteins were reduced by 5 mM TCEP and alkylated by 2 mM MMTS at room temperature for 30 min. Acrylamide/bisacrylamide (40%, 29:1, v/v), 10% (w/v) APS, and 100% TEMED

were then applied to the sample to polymerize as a gel directly in the microcentrifuge without electrophoresis. The gel was cut into small pieces, washed several times (0.1 M TEABC in 50% (v/v) ACN) and subjected to tryptic digestion (10:1, protein/trypsin, w/w) in 25 mM TEABC overnight at 37 °C. Peptides were extracted from the gel using sequential extraction with 25 mM TEABC, 0.1% (v/v) TFA in water, 0.1% (v/v) TFA in ACN, and 100% ACN. The extracted peptides were concentrated in a SpeedVac (Thermo Savant SC210A, Holbrook, NY), desalted by using C18 ZipTip (Millipore; Cambridge, Ontario, Canada), and subjected to LC-MS/MS analysis.

LC-MS/MS Analysis—Peptide samples were reconstituted in 0.1% (v/v) FA in H_2O and analyzed by Waters Q-TOF[TM] Premier (Waters Corp., Milford, MA). Samples were injected into a 20-mm × 180-μm trap column, separated by 200-mm × 75 mm Waters1 ACQUITY 1.7 mm BEH C18 column using a nanoACQUITY Ultra Performance LC[TM] system (Waters Corp., Milford, MA), and eluted with a linear gradient of 0–80% of 0.1% (v/v) FA in ACN for 120 min at 300 nl/min. MS was operated in electrospray ionization positive V mode with a resolving power of 10,000. A NanoLockSpray[TM] source (Waters Corp., Milford, MA) was used for accurate mass measurements, and the lock mass channel was sampled every 30 s. The mass spectrometer was calibrated with a synthetic human [Glu1]-Fibrinopeptide B solution (1 pmol/μl; Sigma Aldrich) delivered through the NanoLockSpray source. Data acquisition was operated in the data-directed analysis mode to automatically switch between a full MS scan (m/z 400–1600, 0.6 s) and three MS/MS scans (m/z 100–1990, 1.2 s for each scan) sequentially on the three most intense ions present in the full MS scan.

Protein Identification and Label-free Quantification—The peak list resulting from MS/MS spectra was exported to mgf format by Mascot Distiller v2.1.1.0. The datasets were batch-searched and combined-searched by Mascot v2.2 (Matrix science, London, United Kingdom) against International Protein Index (IPI) human database (34) (v3.29, 68161 sequences) from the European Bioinformatics Institute using the following constraints: only tryptic peptides with up to two missed cleavage sites were allowed; 0.3-Da mass tolerances for MS and 0.1-Da mass tolerances for MS/MS fragment ions. Methylthio (Cys) and oxidation (Met) was specified as variable modifications. Only unique peptides with scores ≥35 ($p < 0.05$) were confidently assigned. In each MS/MS spectrum, a total of at least four b- and y-ions were observed. To evaluate the false discovery rate in protein identification, we performed a decoy database search against a randomized decoy database created by Mascot using identical search parameters and validation criteria. The search results in Mascot were exported in eXtensive Markup Language data format (XML). The MS/MS spectra and assignment for single peptide identification are included in supplemental Fig. 1.

For label-free quantification, data analysis was performed by our recently developed IDEAL-Q software (32). The raw data files, from Waters Q-TOF Premier were converted into files of mzXML format by masswolf v4.0. IDEAL-Q performs quantitation analysis using spectral data in mzXML format and Mascot search result in XML format. The abundance of a peptide was determined by the extracted ion chromatography (XIC) and further normalized by XIC of the internal standard peptide. The protein ratio was determined by a weighted average of the peptide ratios, where the weight of each peptide ratio is determined by the sample abundance of the corresponding peptide.

Protein Annotation—For subcellular localization, molecular function annotations and information linked to cancer, all the proteins identified in this study were analyzed using the Ingenuity Pathway Analysis Knowledge Base, MetaCore[TM], Human Protein Reference Database, and the Gene Ontology consortium. To predict the position of transmembrane helices and signal peptides, the amino acid sequence of every identified protein was individually searched against the transmembrane hidden Markov model (TMHMM) Server v.2.0 (Center for

Biological Sequence Analysis, Technical University of Denmark) and SignalP3.0 server (35) (Center for Biological Sequence Analysis).

Western Blot Assay—Frozen tissues were thawed and resuspended in lysis solution (0.25 M sucrose, 10 mM Tris-HCl, pH 7.6, 1 mM MgCl$_2$, and 1% SDS) with protease inhibitor mixture (100:1, sample/protease inhibitor, v/v, Calbiochem). Following homogenization (Polytron System PT 1200 E, Luzernerstrasse, Switzerland) on ice, tissue lysate (40 μg) was used for following procedures. For analysis of stomatin-like 2 (STOML2) in plasma, 10 μl plasma was applied for each patient. Proteins were fractionated by 12% SDS-PAGE and transferred to a PVDF membrane (Millipore, Billerica, MA). The membrane was blocked with 5% skim milk in TBS-Tween buffer (25 mM Tris, 190 mM NaCl, and 0.5% (v/v) Tween 20, pH 7.5) and then incubated at 25 °C with the appropriate primary antibody (Claudin 3 antibody, Abcam, Cambridge, MA; Annexin A4 antibody, Abcam; Defensin 1 antibody, Lifespan Bioscience, Seattle, WA; STOML2 antibody, ProteinTech Group Inc., Chicago, IL) at a dilution of 1:1000 for 2 h followed by incubation with peroxidase-conjugated secondary antibody at 25 °C for 1 h. Following washing, the membrane was developed with a chemiluminescence reagent kit (Amersham Biosciences Pharmacia Biotechnology, Inc., Piscataway, NJ) and then exposed to Kodak Bio-Max light film (Sigma-Aldrich, St. Louis, MO). Immunoblot images were analyzed by Imagemaster (Amersham Biosciences, NJ).

Immunohistochemistry (IHC)—The tumor tissue blocks used for IHC were first fixed in 4% paraformaldehyde and then embedded in paraffin. To reduce selection bias, areas of normal colonic epithelium, benign polyps, and adenocarcinoma were reviewed by two independent histopathologists. Sections (5 μm thick) were cut from tissue blocks, mounted on silanized slides (Superfrost, Menzel, Braunschweig, Germany), subsequently deparaffinized with xylene (twice for 10 min each), and rehydrated through ethanol gradient washes as described previously (36). To eliminate the endogenous peroxidase activity, slides were incubated with 3% H$_2$O$_2$ at room temperature for 30 min before heating in a microwave oven for antigen retrieval (10 mM citrate buffer, pH 6.0; 20 min, 700 W). To block nonspecific binding, slides were preincubated with 10% nonimmune goat serum at 37 °C for 30 min. Slides were then incubated with anti-human STOML2 primary antibody (mouse, 1:250 dilution; ProteinTech, Inc., Chicago, IL) for 30 min at room temperature. Following washing with PBS (pH 7.4), slides were incubated with HRP-conjugated anti-mouse IgG secondary antibody (rabbit, 1:2000 dilution; Abcam, Inc., Cambridge, UK) for 30 min at room temperature and then developed using 3,3'-diaminobenzidine (Sigma, St Louis, MO). Sections were counterstained with hematoxylin, washed in running tap water, dehydrated, and mounted in Neo-Mount (Merck, Darmstadt, Germany). Negative control reactions were conducted by omitting the primary antibody.

Scoring of Immunostaining (SI)—Immunostaining was evaluated and scored by two experienced pathologists who were blinded to any knowledge of clinical or pathological parameters and clinical outcome as described previously (37, 38). The percentage of STOML2-positive tumor cells was determined semiquantitatively by assessing the entire tumor section. Expression of the STOML2 protein was categorized as positive or negative and was evaluated according to the simplified H score system (39), which is based on the percentage of cells stained (4, 90–100%; 3, 75–89%; 2, 50–74%; 1, 6–49%; or 0, 0–5%) and the intensity of cell staining (3, strong; 2, moderate; 1, weak; or 0, no cell staining). The two scores are multiplied to obtain the final score. For this study, we defined an SI of 0–9 to indicate negative or low STOML2 protein expression and an SI of 10 or more to indicate positive or high STOML2 expression.

Production of Recombinant STOML2—STOML2 cDNA was obtained by reverse transcription-PCR using total RNA isolated from Colo205 cells (ATCC no. CCL-222) and the following *STOML2*-specific primers, synthesized by MWG-Biotech (Seminole Drive, Hunts-

ville, AL) and based on the *STOML2* gene sequence of GenBank accession number AF190167: STOML2 forward primer, 5'-TTA-CATATGCTTTTG CTGAGGGGCTCTCT-3'; STOML2 reverse primer, 5'-TTTCTCGAGTGTACCCTGGACATCTCTGCT-3'. The PCR amplification product containing nucleotides 97 - 1089 of *STOML2* was subcloned into a pET30b (Novagen, EMD Chemicals Inc., Darmstadt, Germany) expression vector. Sequence analysis was performed using a T7 promoter primer to confirm the *STOML2* sequence. The STOML2 expression plasmid was then transformed into *Escherichia coli* BL21 (DE3) pLysS for recombinant expression. Isopropyl β-d-thiogalacto-pyranoside (IPTG) was used to induce protein expression. The cells were harvested by centrifugation and disrupted by sonication in lysis buffer containing 0.2 M Tris-HCl, pH 7.5; 20% (v/v) glycerol; and 1 mM phenylmethylsulfonyl fluoride at 4 °C. r-STOML2 was purified using a HiTrap^{TM} Chelating HP column (GE Healthcare, Munich, Germany). Expression and purification of the recombinant protein were confirmed with immunoblotting using a mouse monoclonal antibody against the STOML2 protein (ProteinTech Group Inc., Chicago, IL).

ELISA—Briefly, monoclonal anti-human STOML2 (Protein Tech Group Inc., Chicago, IL) in coating buffer (pH 9.5; 15 mmol/l Na$_2$CO$_3$, 35 mmol/l NaHCO$_3$ in distilled water) was added to 96-well microtiter plates (Costar, Illinois, IL) at 100 ng/well and incubated overnight at 4 °C. The plates were washed three times with PBST buffer (PBS with 0.05% Tween-20) and then blocked in blocking buffer (PBST with 2.5% BSA) overnight at 4 °C. Following washing, a twofold dilution of individual plasma samples (50 μl) in blocking buffer (50 μl) was added to each well and incubated at 37 °C for 1 h. Plates were washed three times with PBST buffer and incubated at 37 °C for 1 h with polyclonal rabbit anti-human STOML2 (1:2000; Abcam, Inc.). Plates were washed and incubated at 37 °C for 30 min with HRP-conjugated goat anti-rabbit IgG (1:10,000; Santa Cruz Biotechnology, Santa Cruz, CA). The signal was developed using 3,3,5,5-tetramethylbenzidine (TMB; 100 μl/well; *KBL*, Gaithersburg, MD) as the substrate. To stop the reaction, 1 N HCl (100 μl/well; Sigma-Alderich) was added in each well, and the absorbance was determined at 450 nm with 650 nm as reference filter by spectrophotometer (Molecular Devices, Sunnyvale, CA). All samples were tested in duplicate, and the mean was used for data analysis. A subset of plasma samples and purified recombinant STOML2 proteins (50, 40, 30, 20, 10, and 5 ng/ml) was assayed in every ELISA batch for quality control and quantification, respectively (supplemental Fig. 2). For CEA assay, the plasma CEA levels were determined with a commercially available CEA ELISA kit and protocol (Roche Diagnostics, Mannheim, Germany).

Statistical Analysis—For tissue IHC analysis, associations between protein expression and clinicopathological characteristics were analyzed using the Spearman rank correlation test. For plasma STOML2 levels, relationships were analyzed using the Kruskal-Wallis test and the Mann-Whitney *U* test to analyze differences between individual variables from two groups. The Pearson's Chi-square test was used to analyze the relationship between categorical variables. To determine factors related to overall survival, Cox proportional hazard models (both univariate and multivariate) were used, and the probability was calculated using the Log-rank test by the Kaplan-Meier method. All *p* values were derived from two-tailed statistical tests, and $p < 0.05$ was regarded as statistically significant. The diagnostic potential of a specific marker was evaluated by performing the receiver operating characteristic (ROC) curve analysis and the discriminative efficacy of an individual biomarker was calculated by the area under the ROC curve (AUC).

RESULTS

Analytical Workflow and Performance Assessments

Workflow and Experimental Design—In this study, a simple label-free strategy was designed to quantitatively analyze the
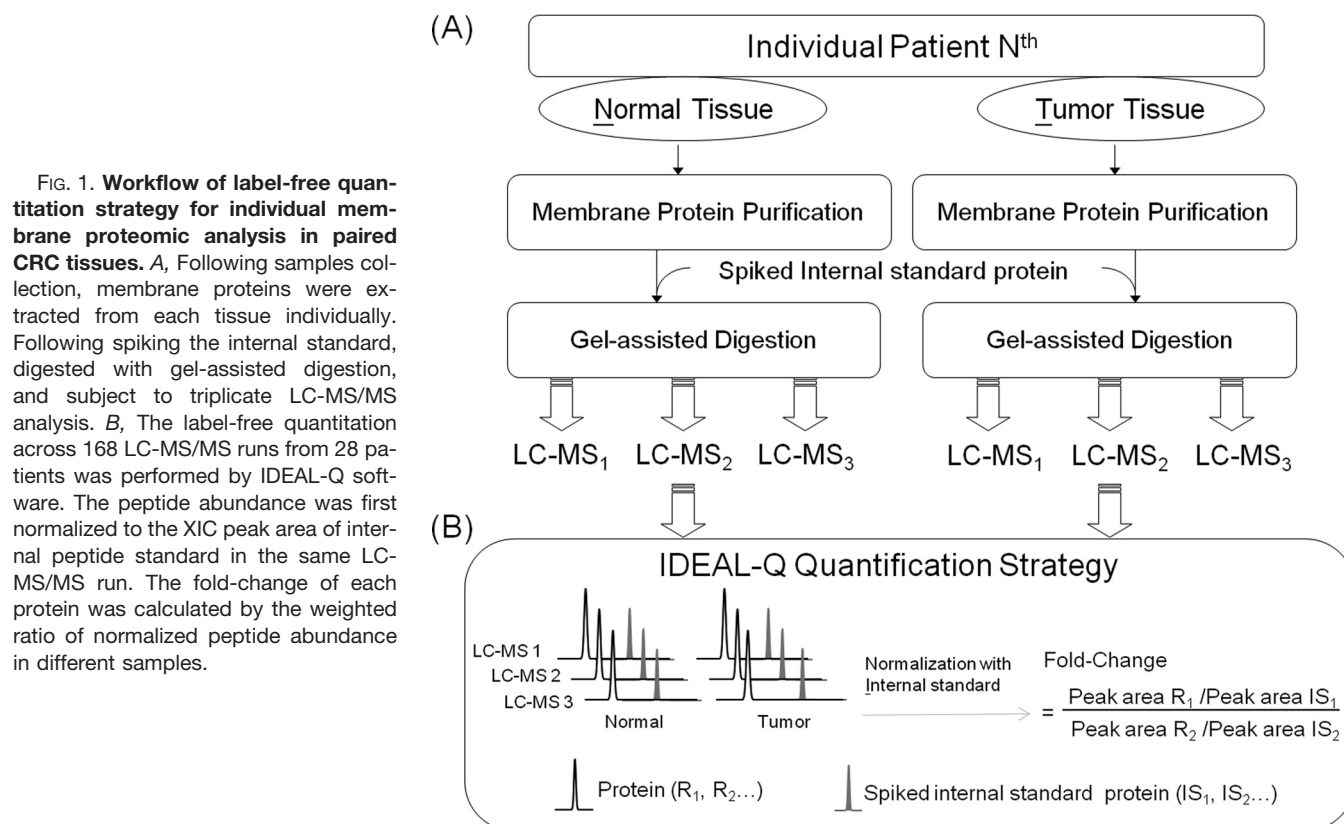
FIG. 1. **Workflow of label-free quantitation strategy for individual membrane proteomic analysis in paired CRC tissues.** *A,* Following samples collection, membrane proteins were extracted from each tissue individually. Following spiking the internal standard, digested with gel-assisted digestion, and subject to triplicate LC-MS/MS analysis. *B,* The label-free quantitation across 168 LC-MS/MS runs from 28 patients was performed by IDEAL-Q software. The peptide abundance was first normalized to the XIC peak area of internal peptide standard in the same LC-MS/MS run. The fold-change of each protein was calculated by the weighted ratio of normalized peptide abundance in different samples.

individual membrane proteome of paired tumor and adjacent normal tissues from 28 CRC patients with Dukes' A, B, C, or D stage. The analytical workflow for individual patients consisted of three steps: (1) membrane protein purification, (2) gel-assisted digestion, and (3) LC-MS/MS analysis (Fig. 1A). Membrane proteins were first purified from paired tumor and adjacent normal tissues, mixed with internal standard protein (BSA), and then subjected to our recently reported gel-assisted digestion (31). When sample along with the spiked BSA was incorporated into a polyacrylamide gel matrix, any interfering components can be removed by in-gel washing steps to ensure efficient enzymatic digestion and LC-MS/MS analysis. To improve reproducibility and reliability of label-free quantitation of individual samples, each batch of extracted peptides was analyzed in triplicate by LC-MS/MS without the fractionation step.

The quantitation analysis was performed by our recently developed software, IDEAL-Q (Fig. 1B) (32), an automated tool for label-free quantitation analysis using an efficient peptide alignment approach and spectral data validation. The software first integrates all protein and peptide identification results from all LC-MS/MS runs, and performed peptide alignment and identification assignment according to the commonly and confidently ($p < 0.05$) identified peptides. The unidentified peptides, which were the result of either a low identification score or an absence of MS/MS sequencing data, can be retrieved based on predicted elution times and

m/z values. To ensure accurate peptide detection and assignment, IDEAL-Q further validated the detected peak clusters by three criteria including signal-to-noise ratio of >3, a correct charge state, and a good isotope pattern. Peptide abundance was determined by peak area of XIC and normalized by XIC area of internal standard peptide in the same LC-MS/MS run. The calculated peptide ratios were further normalized by central tendency normalization (40), and the protein ratios were determined by the weighted average of normalized peptide ratios.

Selection of Internal Standard and Assessment of Reproducibility and Accuracy—To evaluate the reproducibility and accuracy of our method for tissues membrane proteomics, three replicate sets of membrane proteins (20 μg) were purified independently from the same CRC tissue and analyzed. A total of 2152 peptides corresponding to 513 proteins were confidently identified ($p < 0.05$, false discovery rate = 1.1%). We evaluated the quantitation accuracy and precision obtained using different peptides from spiked internal standard protein, BSA (HLVDEPQNLIK, LGEYGFQNALIVR and DAFLGSFLYEYSR), which were chosen based on their different elution times (52.58 ± 0.33 min, 78.99 ± 0.19 min, and 89.13 ± 0.12 min, respectively). In principle, we hypothesized that internal standard peptides that elute at different times can be used to correct chromatographic shifts during long LC gradient. To our surprise, similar accuracy (error = 3–4%) and precision (S.D. = 0.27–0.37) were obtained using single or
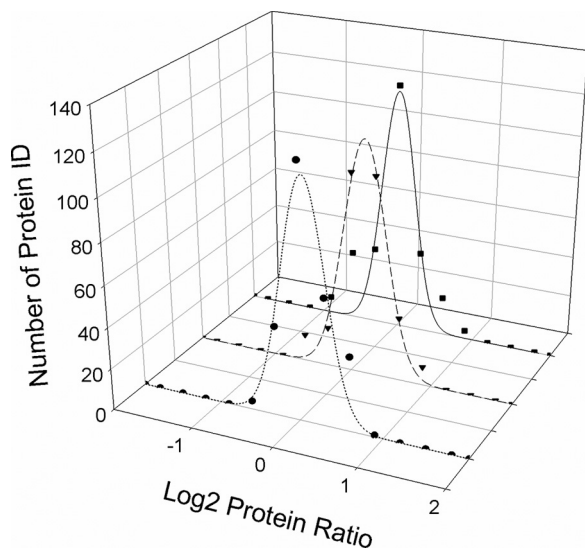
FIG. 2. **The log$_2$ protein ratio distributions obtained from the comparison of three replicate membrane proteins from the same CRC tissue.** All three pair-wise ratios showed narrow normal distributions with mean values of -0.05 ± 0.27, 0.01 ± 0.30, and 0.11 ± 0.37 (95% confidence interval), which are consistent with an expected ratio of 1.0 and relative S.D. of 20.6–29.2% on a linear scale.

combined (two or three) internal standard peptides (supplemental Table 2). Thus, the use of one internal standard peptide, HLVDEPQNLIK, was sufficient to normalize systematic errors.

As shown in Fig. 2, all three pair-wise ratios showed narrow normal distributions with mean values of -0.05 ± 0.27, 0.01 ± 0.30, and 0.11 ± 0.37 (95% confidence interval), which are consistent with an expected ratio of 1.0 and relative S.D. of 20.6–29.2% on a linear scale. Even with the additional membrane protein purification step, the obtained S.D. were comparable with those from previous studies of label-free quantitation of protein expression levels (41, 42). Based on the two-standard deviation model (confidence interval = 95.5%), we considered a difference in abundance of 1.5-fold to indicate a statistically significant degree of higher or lower expression, respectively.

Differential Membrane Proteomics Profiles of Paired Tumor and Adjacent Normal Tissues in CRC Patients

Overall Identification and Quantitation Results—We applied the label-free quantitation strategy to membrane proteomic analysis of paired tumor and adjacent normal tissues from 28 patients. supplemental Table 1 lists the clinical characteristics information of the 28 patients. Based on conventional single LC-MS/MS analysis and database searching, individual patients had only 261–591 protein identifications (Fig. 3A). Because patient heterogeneity leads to the diverse protein expression profiles, the peptide alignment and cross-assignment strategy in IDEAL-Q tool effectively detected almost every identified peptide among LC-MS/MS
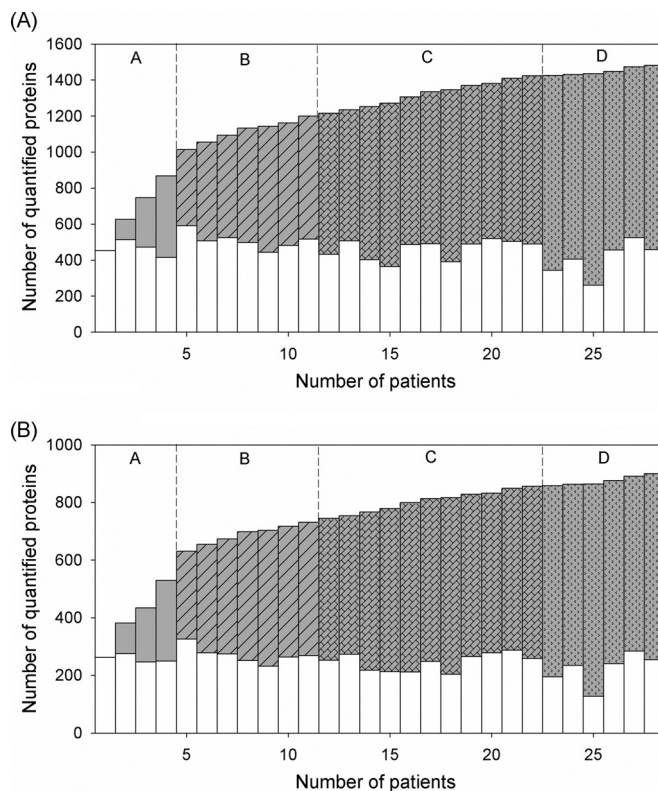

FIG. 3. *A,* **The number of identified proteins distributed among 28 CRC patients.** *B,* The number of quantified proteins in 28 CRC patients. The white bars represent the number of proteins identified or quantified in individual patients. The gray bars represent the accumulative increase in the number of identified or quantified proteins as the number of patients was increased.

dataset from different patients. As shown in the gray bars of Fig. 3A, thus, the number of identified proteins increased from 453 proteins to 1482 proteins (false discovery rate = 2.24%, see detailed identification information in supplemental Table 3) when the number of patient increase.

Under more stringent quantitation criteria by which at least two peptides are required for reliable quantification, 856 proteins were confidently quantified from the 56 tissue samples by IDEAL-Q (Fig. 3B). Among the 856 quantified proteins, 642 were annotated as membrane proteins or membrane-associated proteins including 327 plasma membrane proteins by Gene Ontology, Ingenuity Pathway Analysis Knowledge Base, and TMHMM prediction.

Differentially Expressed Proteins in the Four Different Stages of CRC—To overcome intrinsic intra- and interspecimen variability associated with differing patient characteristics and tissue heterogeneity, quantitative comparison between the tumor and adjacent normal tissues from the same patient is important to minimize the genetic variations. With the criterion of a 1.5-fold change, the quantitation result revealed 216 (Dukes' A), 176 (Dukes' B), 96 (Dukes' C), and 94 (Dukes' D) proteins with higher expression (Ratio >1.5) and 103 (Dukes' A), 111 (Dukes' B), 45 (Dukes' C), and 54 (Dukes'
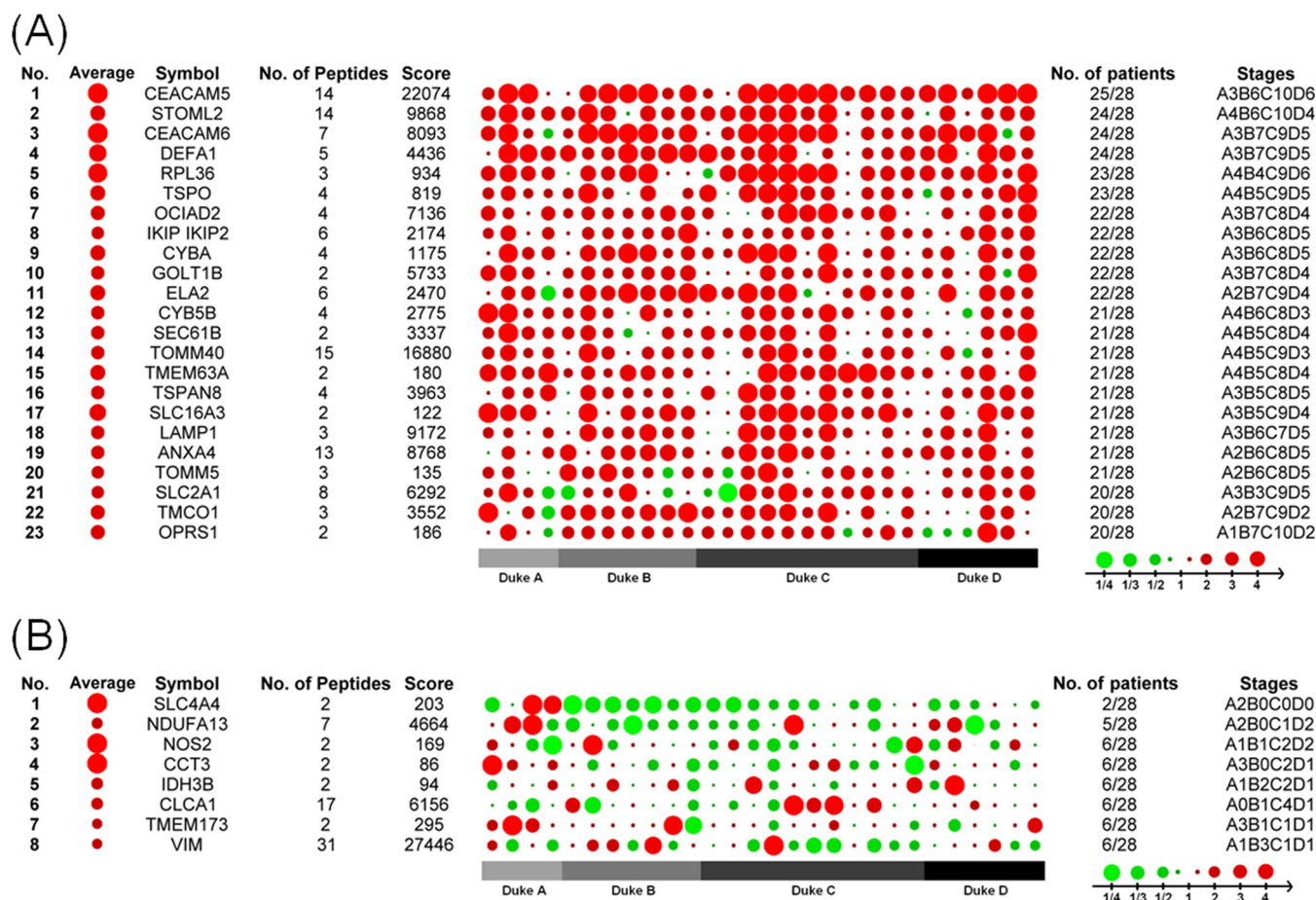
Fig. 4. *A,* Heatmap of proteins that showed > 1. 5-fold up-regulation in ≥ 20 CRC patients. *B,* Heatmap of selected proteins with a significantly elevated average ratio in CRC because of higher expression levels in a small subset of patients. The color and size of dot shown indicates the different extent of up-regulation and down-regulation. The larger size of the dot signifies the greater discrepancy in expression level between tumor and normal tissues. All the patients are organized according to their tumor stage.

D) proteins with lower expression (Ratio <0.67). Among the proteins previously reported as related to CRC, we confidently identified and quantified several carcinoembryonic antigen-related cell adhesion molecules including CEACAM5 (CEA) and CEACAM6; the former is the current prognostic marker used for CRC (8). The representative XICs of CEACAM5 between normal and tumor samples are shown in supplemental Fig. 3. The overexpression of CEA was commonly observed by quantitation of 10 peptides with a total Mascot score of 22,074. CEA showed >1.5-fold higher expression in ≥ 80% of CRC patients (80% of Dukes' A, 85.7% of Dukes' B, 90.9% of Dukes' C, and 100% of Dukes' D). In addition to CEA, the differential expression of other CEACAM family members, such as CEACAM1, CEACAM6, CEACAM7, and CEACAM8, were also observed in our study, as these proteins had >1.5-fold higher expression in 67.9%, 85.7%, 35.7%, and 35.7% of patients, respectively.

We further extracted proteins with high occurrence (≥ 20 patients) of overexpression from four stages (Fig. 4A; Table I). Table I lists their detailed information for these proteins including Mascot score, subcellular localization, and number of

transmembrane helices as well as expression in cell lines, tissues and serum. The color and size of dot shown in Fig. 4A indicates the different extent of fold-change. The magnitude of the average ratio of each protein did not closely correlate with the number of patients with elevated protein levels (Fig. 4A).

The comparison of individual ratio and average ratio indicated that the traditional way of pooling samples from different patients may identify misleading biomarker candidate. The protein represented in Fig. 4B, have significantly high average ratios obtained from the 28 paired tissues. However, only a few patients had dramatically elevated levels, which influenced the overall average ratios of the pooled sample; the expression levels in the remaining samples were unchanged or even slightly down-regulated. Therefore, pooled results do not adequately represent each individual, emphasizing the superiority of personalized membrane proteomics. Personalized membrane proteomics profiles of individual patients can differentiate among biomarker candidates by avoiding the use of potentially misleading average ratios.

Validation of Selected Proteins by Western Blotting—To further validate the differential membrane proteomic profiles

TABLE I

Top 23 proteins with 1.5-fold higher expression in ≥20 CRC patients and their detailed information including identification confidence, subcellular localization, and number of transmembrane helices (TMH) as well as expression in cell lines, tissues and serum

No	Symbol	Description	No. of Patients with up-regulation	Location[a]	TMH[b]	Signal peptide[c]	Plasma/Serum[d]	Large Intestine[d]	COLO205[d]	HCT-116[d]	HCT-15[d]	HT29[d]	KM-12[d]	SW-620[d]	Expressed in CRC Tissue[e]
1	CEACAM5	Carcinoembryonic antigen-related cell adhesion molecule 5 precursor	25	PM	0	Yes	x	x					x		x
2	STOML2	Stomatin-like protein 2	24	PM	1	Yes		x	x	x	x	x	x	x	
3	CEACAM6	CEACAM6 Carcinoembryonic antigen-related cell adhesion molecule 6 precursor	24	PM	0	Yes							x		x
4	DEFA1	Neutrophil defensin 1 precursor	24	Extracellular region	0	Yes									x
5	RPL36	60S ribosomal protein L36	23	Cytoplasm	0	No			x	x	x	x	x	x	
6	TSPO	Peripheral benzodiazepine receptor	23	OM	3	Yes		x	x	x	x	x	x	x	x
7	OCIAD2	OCIA domain containing 2 isoform 1	22	OM	0	No			x	x	x	x	x	x	
8	IKIP	IKIP2	22	OM	0	No									
9	CYBA	Cytochrome b-245 light chain	22	PM	3	Yes		x	x	x	x	x	x	x	
10	GOLT1B	Vesicle transport protein GOT1B	22	OM	3	Signal anchor		x	x	x	x	x	x	x	
11	ELA2	Leukocyte elastase precursor	22	Extracellular region	1	Yes	x								
12	CYB5B	Cytochrome b5 outer mitochondrial membrane precursor	21	OM	1	No		x	x	x	x	x	x	x	
13	SEC61B	Protein transport protein Sec61 subunit beta	21	OM	1	No			x	x	x	x	x	x	
14	TOMM40	Isoform 1 of Probable mitochondrial import receptor subunit TOM40 homolog	21	OM	0	No			x	x	x	x	x	x	
15	TMEM63A	Transmembrane protein 63A	21	PM	11	Signal anchor			x	x	x	x	x	x	
16	TSPAN8	Tetraspanin-8	21	PM	4	Yes		x	x	x	x	x	x	x	x
17	SLC16A3	Monocarboxylate transporter 4	21	PM	12	Yes			x	x	x	x	x	x	x
18	LAMP1	Lysosomal-associated membrane protein 1	21	OM	2	Yes	x	x	x	x	x	x	x	x	x
19	ANXA4	ANXA4 protein	21	PM	0	No		x	x	x	x	x	x	x	x
20	TOMM5	Uncharacterized protein C9orf105	21	Unknown	0	No									
21	SLC2A1	Solute carrier family 2, facilitated glucose transporter member 1	20	PM	12	Yes	x	x	x	x	x	x	x	x	x
22	TMCO1	Isoform 1 of Transmembrane and coiled-coil domain-containing protein 1	20	OM	2	Yes			x	x	x	x	x	x	
23	OPRS1	Isoform 3 of Sigma 1-type opioid receptor	20	PM	1	Yes		x	x	x	x	x	x	x	

[a] The location is annotated by Gene Onotology and Ingenuity Pathway Analysis Knowledge Base. PM indicates plasma membrane and OM indicates organelle membrane.
[b] TMH (transmembrane helix) is predicted by TMHMM Server v.2.0.
[c] Signal peptide is predicted by SignalP 3.0 Server.
[d] The data are obtained from Ingenuity Pathway Analysis.
[e] The expression of proteins in colorectal cancer tissues are obtained in Human Protein Reference Database.
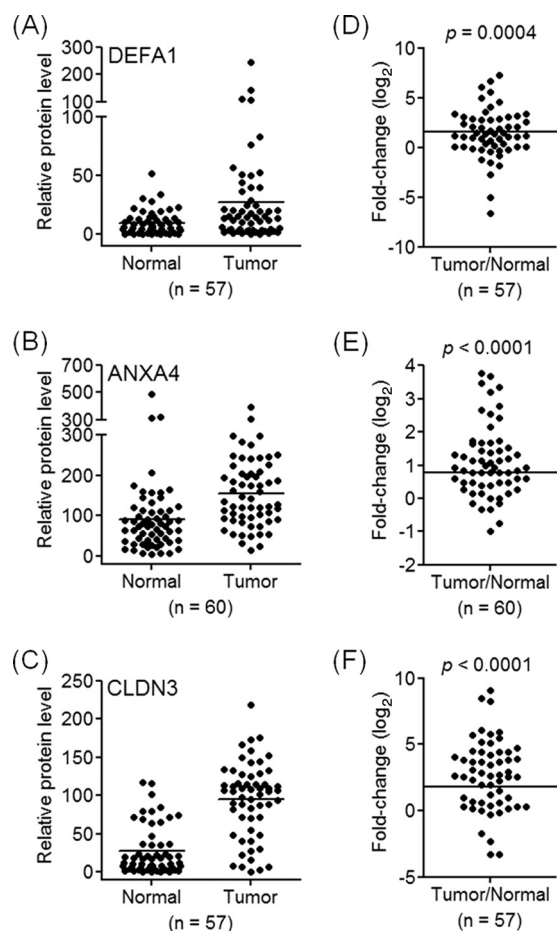
FIG. 5. **Western blot validation of *A,* DEFA1, *B,* ANXA4, and *C,* CLDN3 expression levels in tissue samples.** The fold-changes of (*D*) DEFA1, (*E*) ANXA4, and (*F*) CLDN3 in tumor *versus* normal tissues were evaluated by two-sided *t* test ($p < 0.05$). The raw data points were presented as scatter plot and the mean values were indicated.

in tissues obtained from our label-free strategy, we examined the expression levels of several candidate proteins in tissues from 60 patients by Western blotting. Neutrophil defensin 1 (DEFA1), annexin A4 (ANXA4), and claudin 3 (CLDN3) were selected based on several criteria including (1) structural characterization as plasma membrane proteins, which may enable their use as serological biomarkers; (2) their potential roles in contributing to CRC diagnosis, and (3) the availability of commercial antibodies.

As shown in Fig. 5*A–C* (supplemental Fig. 5), the expression levels were 9.1 ± 10.1 for DEFA1 in normal tissue, and 27.4 ± 42.2 in tumor tissue. The expression levels of ANXA4 were 90.2 ± 83.5 in normal tissue and 154.4 ± 82.7 in tumor. The CLDN3 expression levels were 27.1 ± 31.8 in normal and 94.5 ± 49.0 in tumor tissue. As shown in Fig. 5*D–F*, statistical analysis revealed that the mean of expression level of DEFA1, ANXA4, and CLDN3 were higher (threefold, $p = 0.0004$, 1.7-fold, $p < 0.0001$, and 3.5-fold, $p < 0.0001$, respectively; by two-sided *t* test) in tumor *versus* normal tissues. The fold-

change in expression levels of the three proteins obtained by Western blot for these patients were similar to the higher expression in cancerous tissue (DEFA1: 5.1 ± 4.7, ANXA4: 2.4 ± 1.2, CLDN3: 2.6 ± 2.5) as measured by the MS-based label-free quantification strategy.

Validation of STOML2 as a Candidate Marker in Early CRC Detection and Prognosis—To search for proteins with potential utility in early detection and/or prognosis of CRC, in addition to the above-mentioned criteria, we further filter proteins with criteria of (1) high frequency of overexpression in both early stages and advanced stages of CRC and (2) structural characteristic as secreted proteins, which may enable their use as serological biomarkers. Stomatin-like 2 (STOML2) was overexpressed in 24 CRC patients (Fig. 4 and Table I). Elevated levels of STOML2 had been reported in various tumor types (37, 43–45), suggesting that STOML2 might play an important role in tumorigenesis. As for its association with CRC, however, it was only found in the large intestine, and expression levels of STOML2 in CRC patients have not been investigated.

To confirm the high expression of STOML2, tumor tissues from 205 CRC patients were collected for immunohistochemical (IHC) analysis. Fig. 6*A–C* shows representative cases that harbored both tumor and nontumor cells. Little or weak staining of STOML2 on nontumor epithelial cells was found in most of the samples examined. In contrast, the tumor tissues showed moderately to strongly positive reactions to STOML2, in which the staining of STOML2 mainly localized in the plasma membrane of the tumor cells (Fig. 6*D–E*). Careful inspection of stained sections containing benign polyp materials revealed that most of the benign cells were weakly stained with anti-STOML2 antibody, as compared with the highly stained tumor cells (Fig. 6*F*). In addition, intense and high coverage of cell surface expression of STOML2 was observed in all CRC stages (intensity 3+ and staining cell percentage 100%; Fig. 6*G–J*).

A high level of STOML2 expression, *i.e.* a SI value of ≥10 (see Experimental procedures), occurred consistently in 96% of the 205 patients (Table II). Among the 205 CRC tissue sections examined, 205 sections harbored nontumor epithelial cells, of which 43% (88/205) were positive for STOML2 expression. The percentage of positive staining in malignant tissues was significantly increased as compared with that in normal tissues (Fisher exact test, $p < 0.001$). To further determine whether the overexpression of STOML2 occurred in premalignant lesions of CRC, we compared the SI value between normal and benign polyp tissues. A total of 184 sections contained benign polyp adenoma; positive STOML2 expression was significantly higher (62%, 114/184; Fisher exact test, $p < 0.001$) in benign polyp tissue *versus* normal tissue. Based on this observation, we hypothesize that overexpression of STOML2 is an early event in CRC development, which needed larger-scale clinical studies to verify this speculation. It is noted that there was no
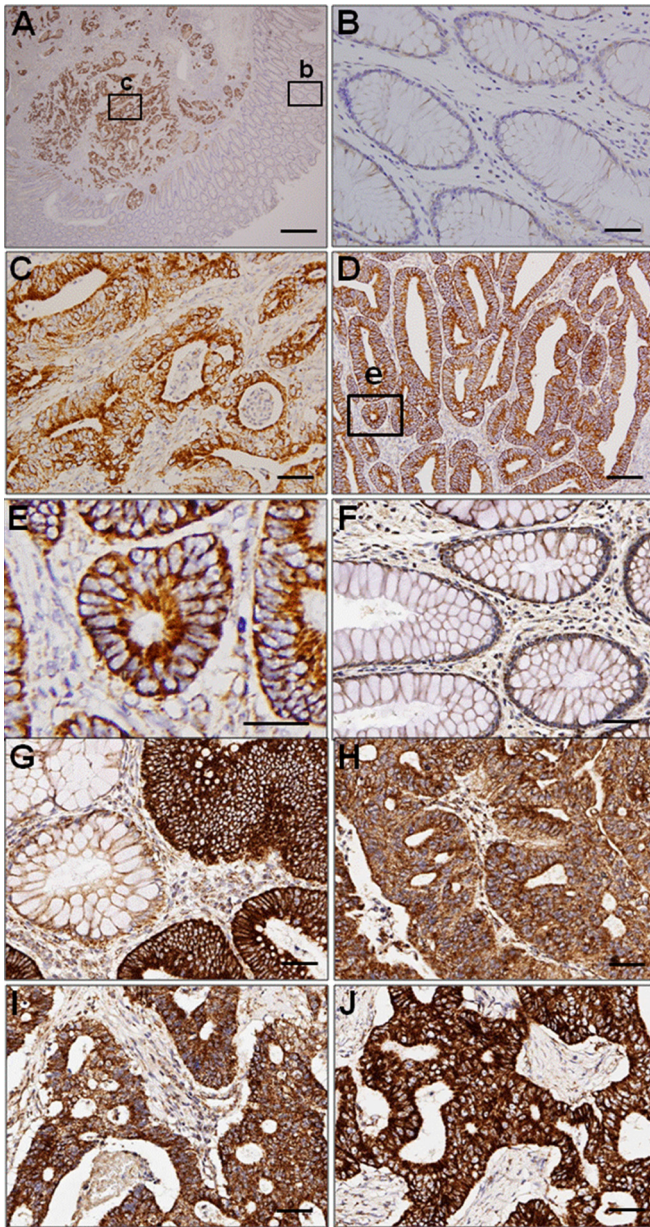
FIG. 6. **IHC analysis of STOML2 expression in CRC tissues.** Representative IHC staining patterns of STOML2 are presented. (A–C) A, Expression of STOML2 in a CRC specimens containing both tumor and nontumor cells. STOML2 was strongly expressed in tumor cells but not in neighboring nontumor epithelium cells. The boxed area for nontumor (b) and tumor (c) cells were enlarged and shown in (B) and (C), respectively. D, Membrane localization of STOML2 overexpressed in tumor cells. The boxed area in (D) was enlarged and shown in (E). F, STOML2 expression in tissue sections containing benign epithelium cells. (G–J) Intense STOML2 expression in tumor cells of CRC specimens from patients with Dukes' stage A - D (intensity 3+ and staining cell percentage 100%). scale bar: 500 μm in (A); 50 μm in (B and C); 100 μm in (D, F–J); or 5 μm in (E).

statistical relationship between STOML2 expression and the clinicopathological parameters examined in the present study (Table III), including histological grade ($p = 0.451$),

tumor stage ($p = 0.232$), lymph node metastasis ($p = 0.343$), distal metastasis ($p = 1.000$).

Prognostic Implications of Tissue STOML2 Expression—Among the 205 CRC patients, 154 patients showed valid survival data. We conducted univariate and multivariate analyses of several prognostic factors (gender, age at onset, tumor stage, nodal stage, metastasis stage, overall stage, differentiation grade, CEA level, and STOML2 expression) for these 154 patients on overall survival using the Cox proportional regression models. Several factors displayed statistically significance in univariate analysis (Table IV); however, following multivariate analysis, only the STOML2 expression ($p = 0.029$) and the metastasis stage ($p < 0.001$) were found to be independent poor prognostic indicators for overall survival (Table IV). Further analysis using Kaplan-Meier plot showed that the 5-year overall survival for patient subgroups stratified by STOML2 expression levels (SI <10 and ≥10) were 75 and 42%, respectively; this difference was statistically significant using a log-rank test ($p = 0.047$; supplemental Fig. 4). Mean survival period was 34.77 ± 2.03 months in patients with high STOML2 expression, whereas 53.67 ± 3.46 months was obtained for patients with low STOML2 expression.

The Diagnostic Value of Plasma STOML2 Protein—We hypothesized that STOML2, a transmembrane protein with a signal peptide, may be secreted into the blood stream as a potential serologic CRC biomarker, although its presence in serum had not been confirmed (Table I). Therefore, we developed an in-house ELISA (see supplemental Fig. 2) to analyze the plasma levels of STOML2 protein from 70 CRC patients and 70 healthy controls (see "Experimental Procedures"). The mean plasma level of STOML2 was ~twofold higher in the CRC patients (5.61 ng/ml) as compared with that in the healthy controls (2.77 ng/ml) (Student's t test, $p < 0.01$, Fig. 7A). To further evaluate the diagnostic potential, an ROC curve was constructed for the plasma STOML2 and CEA level (Fig. 7B). STOML2 and CEA had statistically significant AUC values of 0.74 and 0.69, respectively, demonstrating the potential of STOML2 as a novel candidate CRC biomarker. When 3.5 ng/ml, determined by the optimal Youden's index, was set as a cutoff value, overexpression of STOML2 was found in 37.1% (26 of 70) of normal controls and 71% (50 of 70) of CRC patients. Combining data from both markers led to a further increase in the AUC to 0.77 (Fig. 7B).

Interestingly, the analysis of blood samples from CRC patients revealed that STOML2 and CEA are highly expressed to varying degrees among CRC stages. Many patients (20/29; 69%) with early-stages CRC exhibited high STOML2 plasma levels above the cutoff limit of 3.5 ng/ml, whereas the CEA levels of these patients were mostly below the standard cutoff limit of 5 ng/ml (Fig. 7C). The mean expression level of CEA increased substantially in patients with early-stage CRC as compared with in normal controls (Student t test, $p < 0.001$; Fig. 7D). Elevated STOML2 plasma levels, which were similarly distributed among patients with early-stage and ad-

TABLE II
Expression of STOML2 in normal, benign and malignant colorectal tissues

Characteristics	Test Number	Number of Patient (%)				p Value[c]
		STOML2 (+)[b]		STOML2 (-)[b]		
Tissue statue						
Normal epithelium	205	88	43%	117	57%	<0.001
Benign polyp adenoma[a]	184	114	62%	70	38%	
Malignant carcinoma	205	197	96%	8	4%	
Normal epithelium	205	88	43%	117	57%	<0.001
Benign polyp adenoma[a]	184	114	62%	70	38%	
Normal epithelium	205	88	43%	117	57%	0.001
Malignant carcinoma	205	197	96%	8	4%	
Benign polyp adenoma[a]	184	114	62%	70	38%	<0.001
Malignant carcinoma	205	197	96%	8	4%	

[a] 21 slides were examined but excluded because they lacked benign polyp tissue.
[b] The expression of STOML2 is represented on the staining score (SI). SI from 0 to 9 to indicate negative STOML2 protein expression and a SI of 10 or more to indicate positive STOML2 expression.
[c] Fisher exact test.

TABLE III
Association between expression levels of STOML2 in tissue and clinicopathologic characteristics of 205 CRC patients

Characteristics	Test Number	Number of Patient (%)				p Value[b]
		STOML2 (+)[a]		STOML2 (-)[a]		
Age (years)						0.013
≥60	133	129	97.0%	4	3.0%	
<60	72	63	87.5%	9	12.5%	
Gender						0.392
Male	108	103	95.4%	5	4.6%	
Female	97	89	91.8%	8	8.2%	
Histological grade						0.451
Well differentiation	21	21	100.0%	0	0.0%	
Moderate differentiation	154	143	92.9%	11	7.1%	
Poorly differentiation	30	28	93.3%	2	6.7%	
Tumor stage						0.232
Early stage (stage I-II)	33	29	87.9%	4	12.1%	
Late stage (stage III-IV)	172	163	94.8%	9	5.2%	
Lymph node metastasis (TNM-N stage)						0.343
TNM-N0	95	86	90.5%	9	9.5%	
TNM-N1	43	41	95.3%	2	4.7%	
TNM-N2	52	50	96.2%	2	3.8%	
TNM-N3	15	15	100.0%	0	0.0%	
Distal metastasis (TNM-M)						1.000
No metastasis	146	137	93.8%	9	6.2%	
Distant metastasis	59	55	93.2%	4	6.8%	
CEA concentration						0.061
≥5 ng/ml	91	89	97.8%	2	2.2%	
< 5 ng/ml	114	103	90.4%	11	9.6%	
Total	205	192	93.7%	13	6.3%	

[a] By simplified H score system.
[b] By Fisher exact test.

vanced-stage CRC, did not show a good correlation with tumor stage ($p = 0.97$).

When cutoff values of 5 ng/ml for CEA and 3.5 ng/ml for STOML2 were applied, the overall diagnostic sensitivity of STOML2 and CEA at all stages were 71% and 40% (Table V), respectively. In contrast to CEA, which exhibited higher sensitivity values in advanced tumor stages (24/41, 59%), the superior performance of STOML2 was particularly evident for the early-stage carcinoma (TNM stage I and II). The sensitivity of STOML2 was as high as 69%, whereas CEA has low sensitivity of 14%, which is comparable to previous literature

(8). By combining STOML2 and CEA, the sensitivity for detecting early-stage CRC increased to 76%. Based on the observation, overexpression and secretion of STOML2 into blood may be an early event in colorectal carcinogenesis, which may be utilized for noninvasive early detection of CRC.

DISCUSSION

One of the current bottlenecks in clinical membrane proteomics technologies is the small amount of biomaterial and low throughput when dealing with tissue biopsy specimens. Because the complex composition of proteome is incompat-

TABLE IV
Univariate and multivariate Cox regression analysis of the 5-year overall survival in CRC

Univariate Cox regression analysis	Overall survival		
	Hazard Ratio	95% confidence interval	P
Gender			
Male *vs* Female	0.610	0.397–0.938	0.024
Age			
≥60 *vs* <60	1.318	0.826–2.012	0.246
Tumor stage			
T1-T2 *vs* T3-T4	4.264	1.561–11.649	0.005
Nodal stage			
N1–3 *vs* N0	2.521	1.584–4.011	<0.001
Tumor metastasis			
M1 *vs* M0	4.460	2.862–6.951	<0.001
Overall TNM stage			
Stage 3–4 *vs* stage 1–2	3.591	2.062–6.008	<0.001
Differentiation grade			
Moderate, poor *vs* well	1.934	0.843–4.436	0.120
CEA (5 ng/ml)			
Positive *vs* negative	2.038	1.318–3.153	0.001
STOML2 expression			
High *vs* Low	3.211	1.014–10.170	0.047
Multivariate Cox regression analysis	Overall survival		
	Harzard Ratio	95% confidence interval	P
Tumor metastasis			
M1 *vs* M0	4.603	2.949–7.186	<0.001
STOML2 expression			
High *vs* Low	3.626	1.143–11.502	0.029

ible with the limited acquisition speed of mass spectrometer, only a small fraction of highly abundant peptides will be targeted for MS/MS analysis. Thus, large volumes of biomaterials are necessary when additional fractionation strategies are used to profile less-abundant proteins (46, 47). Although these strategies increase the numbers of confidently identified proteins, nevertheless, they create a tradeoff for overall analytical throughput and may also cause lower quantitation accuracy because of the analytical challenge in confident peptide assignment and peak matching when the same protein/peptide is present in different fractions (32).

In this study, our label-free strategy was designed to balance analytical sensitivity and throughput with depth of proteome coverage for personalized membrane proteomic profiles. Because of the intra- and interstage diversity among patients, the individual membrane proteomics profiles had a small overlap (17.6–39.9%) among all patients. When the proposed SEMI label-free strategy was used for effective peptide alignment and cross-assignment, the patient-to-patient diversity increased the number of quantified proteins without fractionation prior to LC-MS/MS. For each patient, <10 μg of isolated membrane proteins was used to obtain ≈1500 proteins (Q-TOF MS) in the membrane proteomics profiles of tumor and adjacent normal tissue, which is comparable to the result generated using multidimensional peptide separation approaches (48). The high sensitivity of our approach was also demonstrated by the confident identification of the current prognostic marker CEACAM 5 (CEA), with a Mascot score of 22,074. To our knowledge, it is the first report regarding the discovery of CEACAM5 using a proteomics strategy. In addition, the new label-free quantitation strategy provided good accuracy (6% error) and reasonable reproducibility (34% relative S.D.) comparable to isotope labeling strategies (31).

AXNA4, DEFA1, and CLDN3 were identified as potential CRC biomarkers using the label-free strategy. Overexpression of ANXA4 occurs in renal clear cell carcinoma (49), clear cell carcinoma of the ovary (50), papillary thyroid carcinoma (51), and pancreatic adenocarcinoma (52). ANXA4 is also regulated by Tiam1 (T-cell lymphoma invasion and metastasis-inducing protein 1), which is a CRC metastasis-related gene (53); however, its functional role in CRC development is yet to be defined. Defensins (including DEFA1 and DEFA3) levels in stool samples were elevated in CRC, adenoma, and upper gastrointestinal cancers (54). Overexpression of defensins was also found in tissues of colorectal adenomas and carcinomas (55). Aberrant claudin expression has been identified in various cancers, such as those originating from the pancreas, bladder, thyroid, fallopian tubes, ovary, stomach, colon, breast, uterus, and the prostate (56). Thus, we hypothesize that elevated levels of these proteins may be a typical observation in various types of cancer.

Stomatin is a member of the highly conserved family of stomatin proteins (57). Overexpression of stomatin-like 2 (STOML2) has been previously reported in several cancers including esophageal squamous cell carcinoma (43), lung cancer (44), laryngeal cancer (37), and endometrial adenocarcinoma (45), but not in CRC. Transfection of a human esoph-
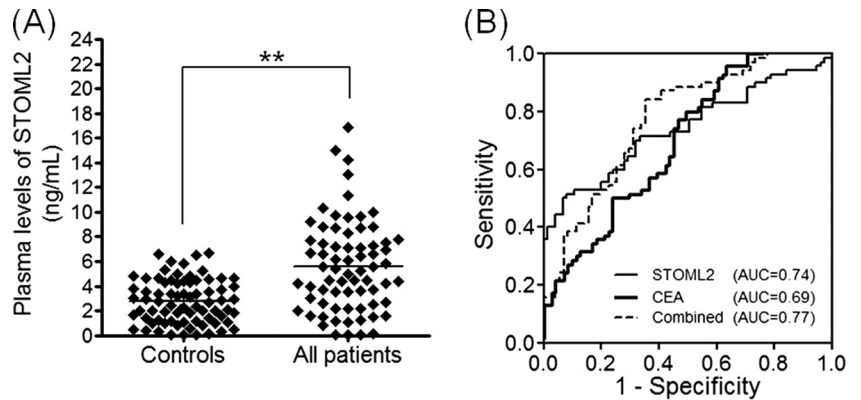
FIG. 7. *A,* **ELISA of the plasma levels of STOML2 in 70 CRC patients and 70 age-matched healthy controls.** *B,* ROC curves of CEA and STOML2 based on the ELISA data shown in (*A*). *C,* Comparison of STOML2 and CEA plasma levels in early- and advanced-stage CRC patients. *D,* ELISA analysis of STOML2 expression in plasma from CRC patients of different stages (early stage: TNM stage I and II, $n = 29$; advanced stage: TNM stage III and IV, $n = 41$) and from healthy controls ($n = 70$). *, $p < 0.01$, **, $p < 0.001$; Student's t test.
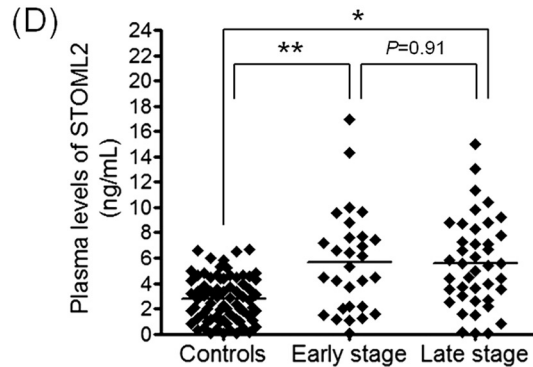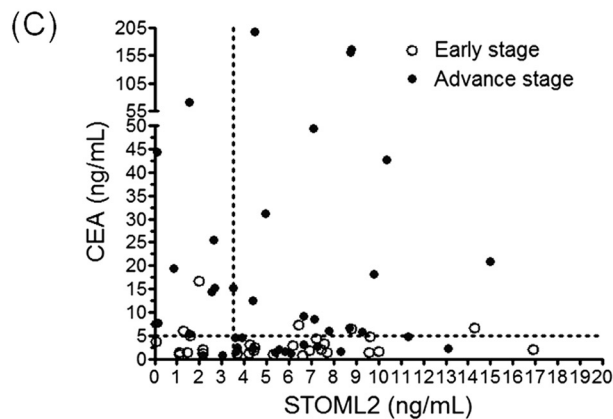
TABLE V
Detection sensitivity of CEA and STOML2 as CRC biomarkers

CRC Stage	Number of patients	(A) CEA[a]	(B) STOML2[b]	Combination
		> 5 ng/ml	>3.5 ng/ml	(A + B)
Early Stage	29	4 (14%)	20 (69%)	22/29 (76%)
Advance stage	41	24 (59%)	30 (73%)	39/41 (95%)
All stages	70	28 (40%)	50 (71%)	61/70 (87%)

[a] Cutoff value was set as 5 ng/ml.
[b] Cutoff value was set as 3.5 ng/ml.

ageal squamous cell carcinoma cell line with antisense STOML2 leads to decreased cell growth, cell adhesion, and tumorigenesis, demonstrating its potential role in controlling tumor growth (58). As one of the most up-regulated proteins in superinvasive cancer cells (59), STOML2 is also associated with decreased overall survival in breast cancer patients when it is expressed at high levels (44). It is regarded as an important player in T-cell activation by ensuring sustained T-cell receptor signaling, making it a potential target for immunomodulation (60). The role of STOML2 in CRC development is, however, still not known (61).

In the study, we presented the first report on the link between STOML2 and its potential applicability for CRC detection and survival prediction. High-level STOML2 expression, *i.e.* an SI value of 10, occurred consistently in almost all CRC patients (94%; 192/205) in every stage (Table II), suggesting the correlation between STOML2 and neoplastic transformation of epithelial cells in colorectum. Elevated level of STOML2 was observed in both CRC tissues and plasma from CRC

patients. The potential use of STOML2 might be best described in comparison with CEA, the most well-established single tumor marker for CRC (7). The overall sensitivity of STOML2 was superior to that of CEA and was comparable to combination of CEA with u-PA or CA 19–9 for screening of CRC (62). CRC detection sensitivity was further improved by the combined use of STOML2 and CEA (87%). Most significantly, more than 70% of patients with early-stage CRC were found to have increased plasma levels of STOML2, suggesting its potential role as an early detection marker in screening asymptomatic patients with CRC.

In conclusion, we demonstrated the feasibility of a simple label-free strategy as a multiplexed quantitative membrane proteomic platform to analyze individual paired tissues in discovery-driven translational cancer research. The proteomic analysis of CRC tissues conducted here provides data for novel candidate biomarkers with potential diagnostic and prognosis value in CRC. Further validation of several plasma membrane proteins in serum samples indicated the potential for tissue membrane proteomics to identify serum markers for noninvasive diagnosis of cancer. It is anticipated that this efficient strategy can be applied to other types of cancer.

[f] To whom correspondence should be addressed: Yu-Ju Chen, Institute of Chemistry, Academia Sinica, Taipei 11529, Taiwan; [g] Department of Chemistry, National Taiwan University, Taipei 10689, Taiwan. Tel.: +886-2-2789-8660; Fax: +886-2-2783-1237; E-mail: yjchen@chem.sinica.edu.tw.

[h] Authors contributed equally to this work.

REFERENCES

1. Weitz, J., Koch, M., Debus, J., Höhler, T., Galle, P. R., and Büchler, M. W. (2005) Colorectal cancer. *Lancet* **365,** 153–165
2. Jemal, A., Siegel, R., Ward, E., Murray, T., Xu, J., and Thun, M. J. (2007) Cancer statistics, 2007. *CA Cancer J. Clin.* **57,** 43–66
3. Kronborg, O., Fenger, C., Olsen, J., Jørgensen, O. D., and Søndergaard, O. (1996) Randomised study of screening for colorectal cancer with faecal-occult-blood test. *Lancet* **348,** 1467–1471
4. Walsh, J. M., and Terdiman, J. P. (2003) Colorectal cancer screening: scientific review. *JAMA* **289,** 1288–1296
5. Smith, R. A., Cokkinides, V., and Eyre, H. J. American Cancer Society guidelines for the early detection of cancer, 2006. *CA Cancer J. Clin.* **56:**11–25, 2006; quiz 49–50
6. Thompson, J. A., Grunert, F., and Zimmermann, W. (1991) Carcinoembryonic antigen gene family: molecular biology and clinical perspectives. *J. Clin. Lab. Anal.* **5,** 344–366
7. Kim, H. J., Yu, M. H., Kim, H., Byun, J., and Lee, C. (2008) Noninvasive molecular biomarkers for the detection of colorectal cancer. *BMB Rep.* **41,** 685–692
8. Wanebo, H. J., Rao, B., Pinsky, C. M., Hoffman, R. G., Stearns, M., Schwartz, M. K., and Oettgen, H. F. (1978) Preoperative carcinoembryonic antigen level as a prognostic indicator in colorectal cancer. *N. Engl. J. Med.* **299,** 448–451
9. Minton, O., and Stone, P. C. (2010) Review: the use of proteomics as a research methodology for studying cancer-related fatigue: a review. *Palliat. Med.* **24,** 310–316
10. Leth-Larsen, R., Lund, R. R., and Ditzel, H. J. (2010) Plasma membrane proteomics and its application in clinical cancer biomarker discovery. *Mol. Cell Proteomics* **9,** 1369–1382
11. Simpson, R. J., Bernhard, O. K., Greening, D. W., and Moritz, R. L. (2008) Proteomics-driven cancer biomarker discovery: looking to the future. *Curr. Opin. Chem. Biol.* **12,** 72–77
12. Sprung, R. W., Jr., Brock, J. W., Tanksley, J. P., Li, M., Washington, M. K., Slebos, R. J., and Liebler, D. C. (2009) Equivalence of protein inventories obtained from formalin-fixed paraffin-embedded and frozen tissue in multidimensional liquid chromatography-tandem mass spectrometry shotgun proteomic analysis. *Mol. Cell Proteomics* **8,** 1988–1998
13. Hwang, S. I., Thumar, J., Lundgren, D. H., Rezaul, K., Mayya, V., Wu, L., Eng, J., Wright, M. E., and Han, D. K. (2007) Direct cancer tissue proteomics: a method to identify candidate cancer biomarkers from formalin-fixed paraffin-embedded archival tissues. *Oncogene* **26,** 65–76
14. Zielinska, D. F., Gnad, F., Wiśniewski, J. R., and Mann, M. (2010) Precision mapping of an in vivo N-glycoproteome reveals rigid topological and sequence constraints. *Cell* **141,** 897–907
15. Uhlén, M., Björling, E., Agaton, C., Szigyarto, C. A., Amini, B., Andersen, E., Andersson, A. C., Angelidou, P., Asplund, A., Asplund, C., Berglund, L., Bergström, K., Brumer, H., Cerjan, D., Ekström, M., Elobeid, A., Eriksson, C., Fagerberg, L., Falk, R., Fall, J., Forsberg, M., Björklund, M. G., Gumbel, K., Halimi, A., Hallin, I., Hamsten, C., Hansson, M., Hedhammar, M., Hercules, G., Kampf, C., Larsson, K., Lindskog, M., Lodewyckx, W., Lund, J., Lundeberg, J., Magnusson, K., Malm, E., Nilsson, P., Odling, J., Oksvold, P., Olsson, I., Oster, E., Ottosson, J., Paavilainen, L., Persson, A., Rimini, R., Rockberg, J., Runeson, M., Sivertsson, A., Sköllermo, A., Steen, J., Stenvall, M., Sterky, F., Strömberg, S., Sundberg, M., Tegel, H., Tourle, S., Wahlund, E., Walden, A., Wan, J., Wernérus, H., Westberg, J., Wester, K., Wrethagen, U., Xu, L. L., Hober, S., and Pontén, F. (2005) A human protein atlas for normal and cancer tissues based on antibody proteomics. *Mol. Cell Proteomics* **4,** 1920–1932
16. Björling, E., Lindskog, C., Oksvold, P., Linné, J., Kampf, C., Hober, S., Uhlén, M., and Pontén, F. (2008) A web-based tool for in silico biomarker discovery based on tissue-specific protein profiles in normal and cancer tissues. *Mol. Cell Proteomics* **7,** 825–844
17. Roessler, M., Rollinger, W., Palme, S., Hagmann, M. L., Berndt, P., Engel, A. M., Schneidinger, B., Pfeffer, M., Andres, H., Karl, J., Bodenmüller, H., Rüschoff, J., Henkel, T., Rohr, G., Rossol, S., Rösch, W., Langen, H., Zolg, W., and Tacke, M. (2005) Identification of nicotinamide N-methyltransferase as a novel serum tumor marker for colorectal cancer. *Clin. Cancer Res.* **11,** 6550–6557
18. Alfonso, P., Núñez, A., Madoz-Gurpide, J., Lombardia, L., Sánchez, L., and Casal, J. I. (2005) Proteomic expression analysis of colorectal cancer by two-dimensional differential gel electrophoresis. *Proteomics* **5,** 2602–2611
19. Rho, J. H., Qin, S., Wang, J. Y., and Roehrl, M. H. (2008) Proteomic expression analysis of surgical human colorectal cancer tissues: up-regulation of PSB7, PRDX1, and SRP9 and hypoxic adaptation in cancer. *J. Proteome Res.* **7,** 2959–2972
20. Ma, Y., Peng, J., Liu, W., Zhang, P., Huang, L., Gao, B., Shen, T., Zhou, Y., Chen, H., Chu, Z., Zhang, M., and Qin, H. (2009) Proteomics identification of desmin as a potential oncofetal diagnostic and prognostic biomarker in colorectal cancer. *Mol. Cell Proteomics* **8,** 1878–1890
21. Xing, X., Lai, M., Gartner, W., Xu, E., Huang, Q., Li, H., and Chen, G. (2006) Identification of differentially expressed proteins in colorectal cancer by proteomics: down-regulation of secretagogin. *Proteomics* **6,** 2916–2923
22. Pei, H., Zhu, H., Zeng, S., Li, Y., Yang, H., Shen, L., Chen, J., Zeng, L., Fan, J., Li, X., Gong, Y., and Shen, H. (2007) Proteome analysis and tissue microarray for profiling protein markers associated with lymph node metastasis in colorectal cancer. *J. Proteome Res.* **6,** 2495–2501
23. Ma, Y. L., Peng, J. Y., Zhang, P., Huang, L., Liu, W. J., Shen, T. Y., Chen, H. Q., Zhou, Y. K., Zhang, M., Chu, Z. X., and Qin, H. L. (2009) Heterogeneous nuclear ribonucleoprotein A1 is identified as a potential biomarker for colorectal cancer based on differential proteomics technology. *J. Proteome Res.* **8,** 4525–4535
24. Krasnov, G. S., Oparina, N., Khankin, S. L., Mashkova, T. D., Ershov, A. N., Zatsepina, O. G., Karpov, V. L., and Beresten, S. F. (2009) [Colorectal cancer 2D-proteomics: identification of altered protein expression]. *Mol. Biol.* **43,** 348–356
25. Alfonso, P., Cañamero, M., Fernández-Carbonié, F., Núñez, A., and Casal, J. I. (2008) Proteome analysis of membrane fractions in colorectal carcinomas by using 2D-DIGE saturation labeling. *J. Proteome Res.* **7,**

4247–4255

26. Prenzel, N., Zwick, E., Leserer, M., and Ullrich, A. (2000) Tyrosine kinase signalling in breast cancer. Epidermal growth factor receptor: convergence point for signal integration and diversification. *Breast Cancer Res.* **2,** 184–190

27. Kufe, D. W. (2009) Mucins in cancer: function, prognosis and therapy. *Nat. Rev. Cancer* **9,** 874–885

28. Hopkins, A. L., and Groom, C. R. (2002) The druggable genome. *Nat. Rev. Drug Discov.* **1,** 727–730

29. Rajcevic, U., Petersen, K., Knol, J. C., Loos, M., Bougnaud, S., Klychnikov, O., Li, K. W., Pham, T. V., Wang, J., Miletic, H., Peng, Z., Bjerkvig, R., Jimenez, C. R., and Niclou, S. P. (2009) iTRAQ-based proteomics profiling reveals increased metabolic activity and cellular cross-talk in angiogenic compared with invasive glioblastoma phenotype. *Mol. Cell Proteomics* **8,** 2595–2612

30. Kristiansen, T. Z., Harsha, H. C., Grønborg, M., Maitra, A., and Pandey, A. (2008) Differential membrane proteomics using 18O-labeling to identify biomarkers for cholangiocarcinoma. *J. Proteome Res.* **7,** 4670–4677

31. Han, C. L., Chien, C. W., Chen, W. C., Chen, Y. R., Wu, C. P., Li, H., and Chen, Y. J. (2008) A multiplexed quantitative strategy for membrane proteomics: opportunities for mining therapeutic targets for autosomal dominant polycystic kidney disease. *Mol. Cell Proteomics* **7,** 1983–1997

32. Tsou, C. C., Tsai, C. F., Tsui, Y. H., Sudhir, P. R., Wang, Y. T., Chen, Y. J., Chen, J. Y., Sung, T. Y., and Hsu, W. L. (2010) IDEAL-Q, an automated tool for label-free quantitation analysis using an efficient peptide alignment approach and spectral data validation. *Mol. Cell Proteomics* **9,** 131–144

33. Wu, C. C., Hsu, C. W., Chen, C. D., Yu, C. J., Chang, K. P., Tai, D. I., Liu, H. P., Su, W. H., Chang, Y. S., and Yu, J. S. (2010) Candidate serological biomarkers for cancer identified from the secretomes of 23 cancer cell lines and the human protein atlas. *Mol. Cell Proteomics* **9,** 1100–1117

34. Kersey, P. J., Duarte, J., Williams, A., Karavidopoulou, Y., Birney, E., and Apweiler, R. (2004) The International Protein Index: an integrated database for proteomics experiments. *Proteomics* **4,** 1985–1988

35. Bendtsen, J. D., Nielsen, H., von Heijne, G., and Brunak, S. (2004) Improved prediction of signal peptides: SignalP 3.0. *J. Mol. Biol.* **340,** 783–795

36. Cattoretti, G., Pileri, S., Parravicini, C., Becker, M. H., Poggi, S., Bifulco, C., Key, G., D'Amato, L., Sabattini, E., Feudale, E., and et al. (1993) Antigen unmasking on formalin-fixed, paraffin-embedded tissue sections. *J. Pathol.* **171,** 83–98

37. Cao, W. F., Zhang, L. Y., Liu, M. B., Tang, P. Z., Liu, Z. H., and Sun, B. C. (2007) Prognostic significance of stomatin-like protein 2 overexpression in laryngeal squamous cell carcinoma: clinical, histologic, and immunohistochemistry analyses with tissue microarray. *Hum. Pathol.* **38,** 747–752

38. Feng Han, Q., Zhao, W., Bentel, J., Shearwood, A. M., Zeps, N., Joseph, D., Iacopetta, B., and Dharmarajan, A. (2006) Expression of sFRP-4 and beta-catenin in human colorectal carcinoma. *Cancer Lett.* **231,** 129–137

39. Ravn, V., Rasmussen, B. B., Højholt, L., Barfoed, M., Heiberg, I., and Thorpe, S. M. (1993) Reproducibility of subjective immunohistochemical estrogen- and progesterone receptor determination in human endometrium. *Pathol. Res. Pract.* **189,** 1015–1022

40. Callister, S. J., Barry, R. C., Adkins, J. N., Johnson, E. T., Qian, W. J., Webb-Robertson, B. J., Smith, R. D., and Lipton, M. S. (2006) Normalization approaches for removing systematic biases associated with mass spectrometry and label-free proteomics. *J. Proteome Res.* **5,** 277–286

41. Ono, M., Shitashige, M., Honda, K., Isobe, T., Kuwabara, H., Matsuzuki, H., Hirohashi, S., and Yamada, T. (2006) Label-free quantitative proteomics using large peptide data sets generated by nanoflow liquid chromatography and mass spectrometry. *Mol. Cell Proteomics* **5,** 1338–1347

42. Old, W. M., Meyer-Arendt, K., Aveline-Wolf, L., Pierce, K. G., Mendoza, A., Sevinsky, J. R., Resing, K. A., and Ahn, N. G. (2005) Comparison of label-free methods for quantifying human proteins by shotgun proteomics. *Mol. Cell Proteomics* **4,** 1487–1502

43. Zhang, L., Ding, F., Cao, W., Liu, Z., Liu, W., Yu, Z., Wu, Y., Li, W., Li, Y., and Liu, Z. (2006) Stomatin-like protein 2 is overexpressed in cancer and involved in regulating cell growth and cell adhesion in human esophageal squamous cell carcinoma. *Clin. Cancer Res.* **12,** 1639–1646

44. Cao, W., Zhang, B., Liu, Y., Li, H., Zhang, S., Fu, L., Niu, Y., Ning, L., Cao, X., Liu, Z., and Sun, B. (2007) High-level SLP-2 expression and HER-2/neu protein expression are associated with decreased breast

patient survival. *Am. J. Clin. Pathol.* **128,** 430–436

45. Cui, Z., Zhang, L., Hua, Z., Cao, W., Feng, W., and Liu, Z. (2007) Stomatin-like protein 2 is overexpressed and related to cell growth in human endometrial adenocarcinoma. *Oncol. Rep.* **17,** 829–833

46. DeSouza, L. V., Grigull, J., Ghanny, S., Dubé, V., Romaschin, A. D., Colgan, T. J., and Siu, K. W. (2007) Endometrial carcinoma biomarker discovery and verification using differentially tagged clinical samples with multidimensional liquid chromatography and tandem mass spectrometry. *Mol. Cell Proteomics* **6,** 1170–1182

47. Elschenbroich, S., Ignatchenko, V., Sharma, P., Schmitt-Ulms, G., Gramolini, A. O., and Kislinger, T. (2009) Peptide separations by on-line MudPIT compared to isoelectric focusing in an off-gel format: application to a membrane-enriched fraction from C2C12 mouse skeletal muscle cells. *J. Proteome Res.* **8,** 4860–4869

48. Slebos, R. J., Brock, J. W., Winters, N. F., Stuart, S. R., Martinez, M. A., Li, M., Chambers, M. C., Zimmerman, L. J., Ham, A. J., Tabb, D. L., and Liebler, D. C. (2008) Evaluation of strong cation exchange versus isoelectric focusing of peptides for multidimensional liquid chromatography-tandem mass spectrometry. *J. Proteome Res.* **7,** 5286–5294

49. Zimmermann, U., Balabanov, S., Giebel, J., Teller, S., Junker, H., Schmoll, D., Protzel, C., Scharf, C., Kleist, B., and Walther, R. (2004) Increased expression and altered location of annexin IV in renal clear cell carcinoma: a possible role in tumour dissemination. *Cancer Lett.* **209,** 111–118

50. Kim, A., Enomoto, T., Serada, S., Ueda, Y., Takahashi, T., Ripley, B., Miyatake, T., Fujita, M., Lee, C. M., Morimoto, K., Fujimoto, M., Kimura, T., and Naka, T. (2009) Enhanced expression of Annexin A4 in clear cell carcinoma of the ovary and its association with chemoresistance to carboplatin. *Int. J. Cancer* **125,** 2316–2322

51. Baris, O., Mirebeau-Prunier, D., Savagner, F., Rodien, P., Ballester, B., Loriod, B., Granjeaud, S., Guyetant, S., Franc, B., Houlgatte, R., Reynier, P., and Malthiery, Y. (2005) Gene profiling reveals specific oncogenic mechanisms and signaling pathways in oncocytic and papillary thyroid carcinoma. *Oncogene* **24,** 4155–4161

52. Shen, J., Person, M. D., Zhu, J., Abbruzzese, J. L., and Li, D. (2004) Protein expression profiles in pancreatic adenocarcinoma compared with normal pancreatic tissue and tissue affected by pancreatitis as detected by two-dimensional gel electrophoresis and mass spectrometry. *Cancer Res.* **64,** 9018–9026

53. Liu, L., Wang, S., Zhang, Q., and Ding, Y. (2008) Identification of potential genes/proteins regulated by Tiam1 in colorectal cancer by microarray analysis and proteome analysis. *Cell Biol. Int.* **32,** 1215–1222

54. Zou, H., Harrington, J. J., Sugumar, A., Klatt, K. K., Smyrk, T. C., and Ahlquist, D. A. (2007) Detection of colorectal disease by stool defensin assay: an exploratory study. *Clin. Gastroenterol. Hepatol.* **5,** 865–868

55. Mothes, H., Melle, C., Ernst, G., Kaufmann, R., von Eggeling, F., and Settmacher, U. (2008) Human Neutrophil Peptides 1–3–early markers in development of colorectal adenomas and carcinomas. *Dis. Markers* **25,** 123–129

56. Hewitt, K. J., Agarwal, R., and Morin, P. J. (2006) The claudin gene family: expression in normal and neoplastic tissues. *BMC Cancer* **6,** 186

57. Wang, Y., and Morrow, J. S. (2000) Identification and characterization of human SLP-2, a novel homologue of stomatin (band 7.2b) present in erythrocytes and other tissues. *J. Biol. Chem.* **275,** 8062–8071

58. Kinzler, K. W., and Vogelstein, B. (1996) Lessons from hereditary colorectal cancer. *Cell* **87,** 159–170

59. Dowling, P., Meleady, P., Dowd, A., Henry, M., Glynn, S., and Clynes, M. (2007) Proteomic analysis of isolated membrane fractions from superinvasive cancer cells. *Biochim. Biophys. Acta* **1774,** 93–101

60. Winawer, S., Fletcher, R., Rex, D., Bond, J., Burt, R., Ferrucci, J., Ganiats, T., Levin, T., Woolf, S., Johnson, D., Kirk, L., Litin, S., and Simmang, C. (2003) Colorectal cancer screening and surveillance: clinical guidelines and rationale-Update based on new evidence. *Gastroenterology* **124,** 544–560

61. Inger, D. B. (1999) Colorectal cancer screening. *Prim. Care* **26,** 179–187

62. Huber, K., Kirchheimer, J. C., Sedlmayer, A., Bell, C., Ermler, D., and Binder, B. R. (1993) Clinical value of determination of urokinase-type plasminogen activator antigen in plasma for detection of colorectal cancer: comparison with circulating tumor-associated antigens CA 19–9 and carcinoembryonic antigen. *Cancer Res.* **53,** 1788–1793